Chemical Science

ROYAL SOCIETY OF CHEMISTRY

EDGE ARTICLE

View Article Online
View Journal | View Issue

Cite this: *Chem. Sci.*, 2025, **16**, 364

All publication charges for this article have been paid for by the Royal Society of Chemistry

Dynamic selection in metallo-organic cube $Cd^{II}_8L_4$ conformations induced by perfluorooctanoate encapsulation†

Yu-Qing Li,‡[a] He Zhao,‡[a] Ermeng Han,[a] Zhiyuan Jiang,*[c] Qixia Bai,[b] Yu-Ming Guan,[b] Zhe Zhang,[b] Tun Wu*[b] and Pingshan Wang *[ab]

Received 18th October 2024
Accepted 22nd November 2024

DOI: 10.1039/d4sc07105k

rsc.li/chemical-science

Metallo-organic cages possess flexibility comparable to that of biological receptors and can alter their conformations to better accommodate guest species due to the dynamic reversibility of the coordination bond. Induced fit is widely accepted involving conformation change of the host, while few definitive examples are related to conformation selection. Herein, we report the generation of metallo-organic cube $Cd^{II}_8L_4$ with two coexisting conformations, which have been fully confirmed by NMR, ESI-MS and single-crystal X-ray diffraction analysis. The specific guest perfluorooctanoate PFOA selectively binds to the active conformer C_{2h}-**1** to form the PFOA⊂C_{2h}-**1** complex. Furthermore, conformer D_2-**2** isomerizes to conformer C_{2h}-**1** in the presence of PFOA, for maximizing the guest binding affinity. This study provides an effective working paradigm for conformation selection, facilitating the understanding of the fundamental mechanism of molecular recognition.

Introduction

Molecular recognition, described as the binding between a substrate molecule and a protein-host, plays an essential role in various biochemical and physiological functions in an organism.[1,2] The "conformational selection" hypothesis postulates that there are a series of discrete conformers for receptors in equilibrium (H and H*), in which the substrate molecule selectively interacts with the active one to form a host–guest complex, subsequently shifting the equilibrium distribution of receptor conformers (Fig. 1).[3,4] It greatly facilitates the comprehensive understanding of molecular recognition in favour of the structure-based drug design, enzymatic catalysis and allosteric regulation of cell signaling.[5–8] Metallo-organic cages (MOCs),[9–18] constructed by the coordination between organic ligands and metal ions, serve as an effective model to simulate the molecular recognition of bio-receptors since their characteristic vacant cavities enclose central guest species, enabling various functional applications including chemical separation,[19–21] sensing,[22–24] mimic catalysis[25–27] and luminescent materials.[28–30]

Moreover, the dynamic reversibility of the dative bond within these three-dimensional (3D) metallo-organic structures provides them with recombination ability in response to external stimuli, specifically metallo-organic cages altering their conformation to fit target guests.[31–40] This guest-induced structural change of metallo-organic cages generally involves an "induced fit" mechanism, in which a guest binds to the receptor in an inactive state, and then undergoes a structural rearrangement into an active model for an optimum fit.[41,42] However, the molecular recognition of metallo-organic cages based on conformation selection is relatively rare and presents a great challenge. An ideal model for conformational selection should meet the criteria that there are two or more pre-existing conformations in equilibrium and that all of them can be detected.[43,44] In general, the conformers that coexist possess

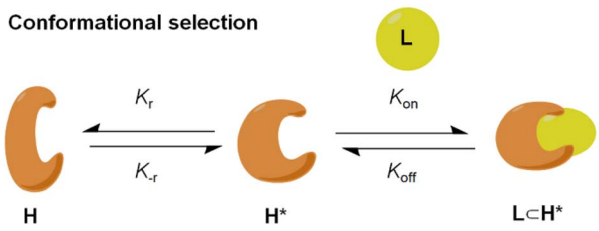

Fig. 1 Conformational selection mechanism involving conformational change of the host.

[a]*Hunan Key Laboratory of Micro & Nano Materials Interface Science, College of Chemistry and Chemical Engineering, Central South University, Changsha 410083, China. E-mail: chemwps@csu.edu.cn*

[b]*Institute of Environmental Research at Greater Bay Area, Key Laboratory for Water Quality and Conservation of the Pearl River Delta, Ministry of Education, Guangzhou University, Guangzhou 510006, China. E-mail: chemwt@gzhu.edu.cn*

[c]*Department of Chemistry, The University of Hong Kong, Hong Kong SAR 999077. E-mail: chemjzy@hku.hk*

† Electronic supplementary information (ESI) available. CCDC 2359196. For ESI and crystallographic data in CIF or other electronic format see DOI: https://doi.org/10.1039/d4sc07105k

‡ These authors contributed equally.

similar energies, presenting great obstacles for their interconversion. Meanwhile, the complete differentiation of different conformers is still highly challenging due to their structural nuances.[45]

Herein, we report the generation of metallo-organic cages $Cd_8^{II}L_4$ in good accordance with the conformation selection mechanism. The self-assembly between tetratopic ligand **L** and Cd^{II} ions afforded metallo-organic cages $Cd_8^{II}L_4$ with the coexistence of two conformers. Conformer **1** is a cuboid metallo-organic cage in which four ligands **L** cap the equatorial faces with C_{2h} symmetry. Differing only in the location orientation of terpyridine units, two parallel ligands **L** together occupy the equatorial faces of conformer **2**, displaying an unprecedented helical cubic structure with D_2 symmetry. Conformer C_{2h}-**1** converts to conformer D_2-**2** at a quite slow rate and an elevated temperature can facilitate this process. Owing to the different cavity volume (**1**: 1263 Å^3, **2**: 867 Å^3) and shape, the inclusion of guest perfluorooctanoate PFOA, classified as a persistent organic pollutant (POP), can only be achieved by conformer C_{2h}-**1** based on the shape and size complementarity. Furthermore, the addition of PFOA into conformer D_2-**2** can shift the equilibrium distribution to conformer C_{2h}-**1** (Scheme 1).

Results and discussion

The tetratopic ligand **L** contains two kinds of terpyridine units: one connects with the 5-position of the lateral pyridine (part A) and the other is substituted on the *para*-position of benzene attached to the central pyridine (part B) (Fig. 2). It was facilely synthesized through successive Suzuki–Miyaura reactions from commercially available 1,5-dibromo-2,4-diiodobenzene (Scheme S1 and Fig. S1–S13†). Part A and part B possess inwardly converging and outwardly extending conformations, respectively, showing geometric complementarity. So, hetero-connection of parts A and B (tpy^A-Cd^{II}-tpy^B) is more favourable than homo-connections (tpy^A-Cd^{II}-tpy^A and tpy^B-Cd^{II}-tpy^B) in terms of geometric conformation. Self-assembled supramolecules are normally favoured thermodynamically over oligomeric or polymeric systems because they are synthesized under thermodynamic conditions, facilitating the formation of finite structures at the expense of increased angle strain. In addition, entropy favours closed structures with a minimum number of components rather than polymeric structures, which involve a far larger number of components.[46,47] So, self-assembly was conducted under thermodynamic conditions: direct reaction of ligand **L** and two equivalents of cadmium nitrate tetrahydrate $Cd(NO_3)_2\cdot 4H_2O$ at 65 °C in a mixed solvent ($CHCl_3$: MeOH = 3 : 4) for 12 h. After cooling to room temperature, excess lithium bis(trifluoromethanesulphonyl)imide ($LiNTf_2$) was added to give a precipitate, which was collected by filtration and further washed with D.I. water and MeOH (Fig. 2a and Scheme S2†). The product conformer **1** was quantitatively obtained as a pale white solid after being dried *in vacuo*. The ^{1}H NMR spectrum of **1** showed a significant upfield shift of H$^{6,6''}$ (part B in ligand **L**) and H^6 (part A in ligand **L**), attributed to the characteristic electron shielding effect caused by the pseudo-

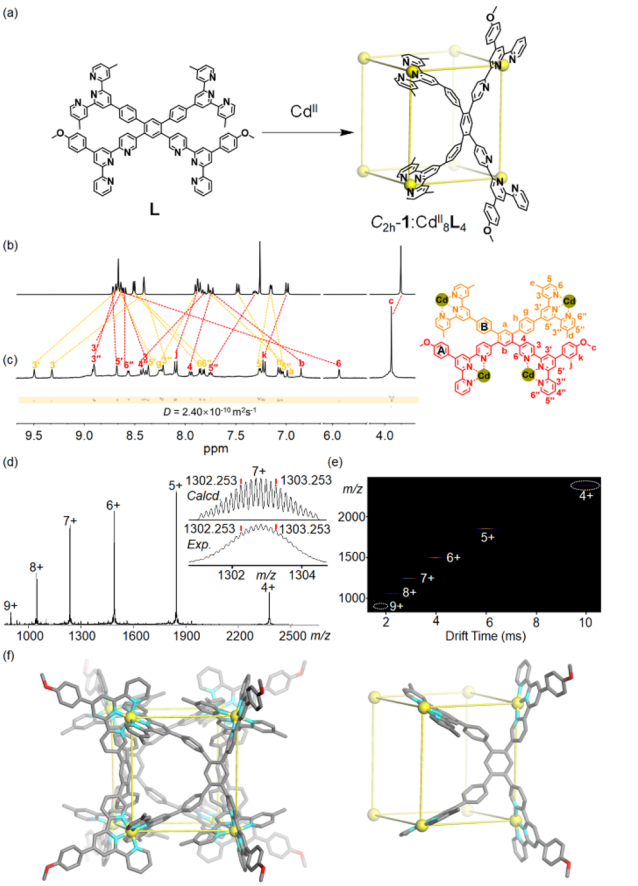

Fig. 2 (a) Self-assembly of metallo-organic cage C_{2h}-**1**. (b) ^{1}H NMR spectrum of ligand **L** (500 MHz, 298 K, $CDCl_3$), (c) ^{1}H NMR and DOSY NMR spectra of metallo-organic cage C_{2h}-**1** (500 MHz, 298 K, CD_3CN-d_3), (d) ESI-MS with the inset showing the isotopic pattern of charge state 7+, (e) TWIM-MS spectra of metallo-organic cage C_{2h}-**1**. (f) Energy-minimized structure and simplified model of C_{2h}-**1**.

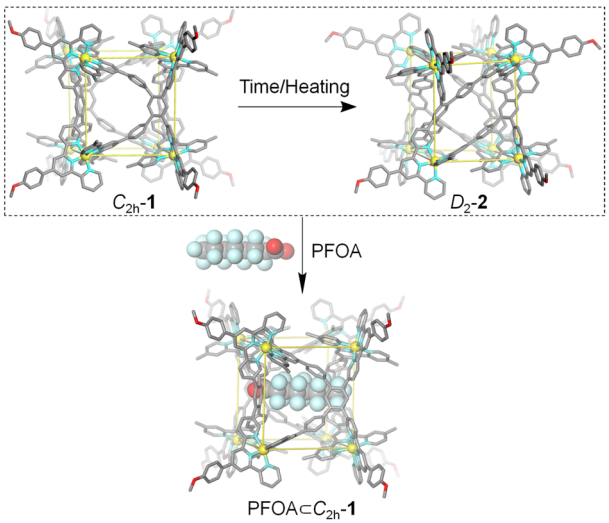

Scheme 1 Conformational change of metallo-organic cages $Cd_8^{II}L_4$ in response to temperature/time and guest PFOA based on the conformational selection mechanism.

octahedral bis(terpyridine) complex.[48] The presence of two singlets of $H^{3',5'}$ and only one singlet of H^{-OMe} attributed to two kinds of terpyridine moieties strongly demonstrated the equivalent environments of each terpyridine unit, indicating the generation of a highly symmetric species (Fig. 2b, f and S14–S16†). Diffusion-ordered ^{1}H NMR spectroscopy (DOSY) analysis confirmed the presence of single discrete species in solution with extracted diffusion coefficient D values of 2.4×10^{-10} m^2 s^{-1} (Fig. 2c and S17†). In addition, electrospray ionization mass spectrometry (ESI-MS) was performed to provide composition information of conformer **1**. It displays a series of multicharged ions from $[Cd^{II}_8\mathbf{L}_4 + 5NTf_2^- + 2NO_3^-]^{9+}$ to $[Cd^{II}_8\mathbf{L}_4 + 10NTf_2^- + 2NO_3^-]^{4+}$, demonstrating the exclusive formation of $Cd^{II}_8\mathbf{L}_4$ type assemblies. It's noted that the experimental isotopic patterns for each charge state agreed well with the calculated distributions (Fig. 2d and S18†). 2D travelling wave ion migration mass spectrometry (TWIM-MS) exhibited a narrow drift time distribution of each charge state for conformer C_{2h}-**1**, ruling out other isomers and conformers (Fig. 2e). The results of NMR, MS and computational simulation strongly indicate a metallo-organic cube with C_{2h} symmetry of conformer **1**. It's noted that self-assembly between ligand **L** and Zn^{II} gives an isostructural metallo-organic cage $[Zn^{II}_8\mathbf{L}_4]$ (Fig. S43 and S44†).

As time went by, an unexpected growth in the number of proton resonances was observed in the ^{1}H NMR spectra of C_{2h}-**1**. Three months later, a brand-new and highly complicated ^{1}H NMR spectrum can be detected, showing four sets of terpyridine signals in the aromatic region along with two singlets derived from methoxy (Fig. 3b and S19–S21†). Its ^{1}H DOSY NMR spectrum confirms that all signals have the same diffusion coefficient D of 2.4×10^{-10} m^2 s^{-1} which is similar to that of conformer C_{2h}-**1** (Fig. 3c and S22†). The identical $Cd^{II}_8\mathbf{L}_4$-composition of metallo-organic cage **2** was further verified by ESI-MS coupled with TWIM-MS (Fig. S23 and S24†). Therefore, it can be concluded that the product self-assembled from ligand **L** and Cd^{II} ion has two conformers (Fig. 3a) with different symmetries and thus different peak patterns in the ^{1}H NMR spectra. Conformational conversion from conformer C_{2h}-**1** to conformer **2** is slow on the NMR timescale, enabling their direct differentiation in ^{1}H NMR spectra. In order to accelerate conformational conversion, the NMR tube of C_{2h}-**1** was heated at 65 °C, achieving a complete transformation to conformer **2** after four weeks. It's noted that conformer C_{2h}-**1** cannot be recovered even by freezing treatment of conformer **2** (208 K, 1 month). The above results illustrate that conformer **2** is thermodynamically preferred compared to metastable and kinetic conformer C_{2h}-**1**.

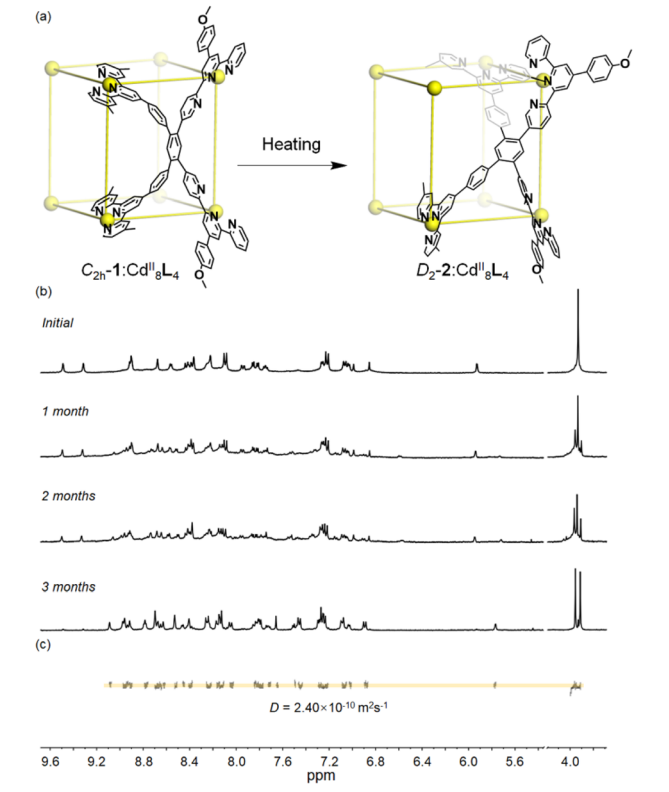

Fig. 3 (a) Conformational conversion from conformer C_{2h}-**1** to conformer **2**. (b) Time-resolved ^{1}H NMR spectra, and (c) DOSY NMR spectra of metallo-organic cage conformer **2** (500 MHz, 298 K, CD_3CN-d_3).

Subsequently, by slow diffusion of isopropyl ether over a month or three days' diffusion of toluene into an acetonitrile solution of the product assembled from ligand **L** and Cd^{II} ions, single crystals suitable for X-ray diffraction (SC-XRD) were achieved (Table S1†). There are two problems in obtaining high-quality crystals: (1) during the crystallization process, gel is always generated and (2) due to the presence of large voids and highly disordered solvents/anions, the reflections in the high θ angle are too weak to obtain completeness and good data/parameter ratios. Fortunately, the satisfactory refinement results are sufficient for the cage structure determination. It revealed a helical cuboid structure in which the eight Cd^{II} ions occupy the vertices. The neighbouring $Cd^{II}\cdots Cd^{II}$ distances were measured to be 11.4–13.5 Å corresponding to the different edges of the cube (Fig. S35†). Along the equatorial plane of the cubic structure, three terpyridine arms (two tpy-A, one tpy-B) in ligand **L** bridge the metal centers and the last one (tpy-B) extends to the opposite plane and coordinates to the metal center on the body diagonal. In this manner, two ligands **L** together form a face of the helical cube which is totally different from the ligand face-capped cuboid metallo-organic cages.[49,50] The solid-state structure of the helical cube shows multiple extended orientations of terpyridine units which is consistent with the increased number of proton resonances in the ^{1}H NMR spectra of conformer D_2-**2** rather than highly-symmetric conformer C_{2h}-**1** with only two kinds of terpyridine units. There are two C_2 axes that are perpendicular to each other and no symmetry plane can be observed, demonstrating the D_2 symmetry of helical cube **2** (Fig. 4). Despite many attempts, only single crystals attributed to D_2-**2** can be detected, probably because it's easier to crystallize in contrast to C_{2h}-**1**.

As we fully confirmed the conformational conversion from C_{2h}-**1** to D_2-**2** and their exact structures, calculations using Forcite of Materials Studio were performed to investigate the energy difference between these conformers. Conformer D_2-**2** is 28.19 kcal mol^{-1} more stable than conformer C_{2h}-**1** (Fig. S39†),

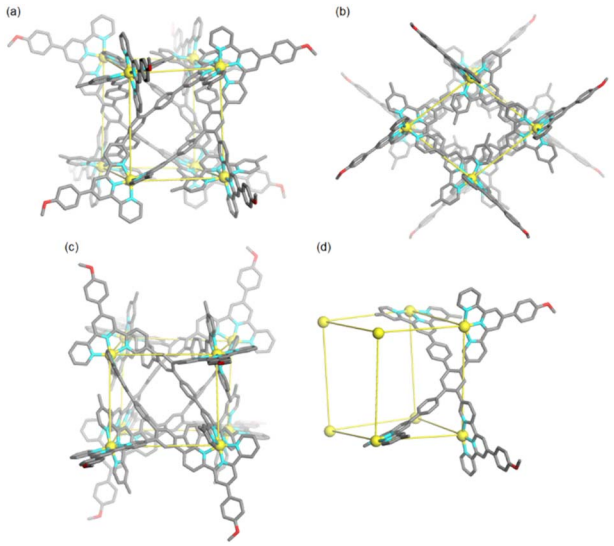

Fig. 4 (a–c) Three views of the single crystal X-ray structure of metallo-organic cage D_2-**2**. (d) The geometrical illustration of metallo-organic cage D_2-**2**.

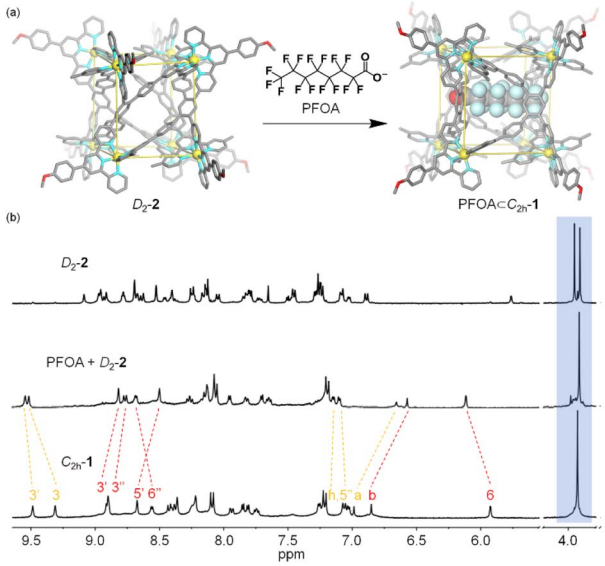

Fig. 5 (a) PFOA-induced conformational selection from D_2-**2** to PFOA⊂C_{2h}-**1**. (b) ^{1}H NMR spectra of (top) D_2-**2**, (middle) D_2-**2** + PFOA, (bottom) C_{2h}-**1** (500 MHz, CD_3CN-d_3, 298 K).

rationalizing the thermodynamically controlled conversion. The cavities of the two conformers (C_{2h}-**1** and D_2-**2**) were well-enclosed by ligand **L**, and the methyl groups of part B further blocked the pores of the two apical vacant planes (Fig. 4b and S36†). Calculated using VOIDOO,[51] the internal cavity volumes of two conformers were different, at 1263 Å^3 and 867 Å^3 for C_{2h}-**1** and D_2-**2**, respectively (Fig. S37 and S38†).

The two conformers C_{2h}-**1** and D_2-**2** may possess drastically different binding affinities toward the same guest due to their different cavity size and shape. So, it's an ideal model for conformational selection, in which a guest will only be encapsulated by one conformation and will not bind to the other at all. Moreover, when accommodating a specific guest, the original equilibrium between the conformers will be broken, leading to the exclusive generation of one kind of host–guest complex owing to the dynamic reversible nature of dative bonds. After screening (Fig. S25–S28†), perfluorooctanoate (PFOA) was found to be a suitable guest. PFOA accumulates in water resources and poses serious environmental and health threats due to its non-biodegradable nature and long environmental persistence time.[52–54] Effective recognition of PFOA by artificial hosts may bring about the sensing or even adsorption materials for PFOA pollutant.[55–57] The addition of excess PFOA into the solution of conformer D_2-**2** resulted in a reduction in the number of terpyridine units from 4 to 2, along with the appearance of only one singlet assigned to methoxy for part A of ligand **L**, strongly indicating the main structure of conformer D_2-**2**'s conversion to conformer C_{2h}-**1**. And, compared to the ^{1}H NMR spectra of conformer C_{2h}-**1**, proton resonance of H^3 on part B of ligand **L** displayed a moderate downfield shift (from 9.31 ppm to 9.51 ppm) and the other signals shifted to the upfield. In addition, ^{19}F NMR signals of the fluorine atoms on C_{2h}-**1** derived from NTf_2^- showed obvious upfield shift with the addition of PFOA, along with the upfield shift and broadening of ^{19}F signals on guest PFOA, which is consistent with previous reports.[58,59] The obvious changes in ^{1}H and ^{19}F NMR spectra were indicative of a molecule of PFOA encapsulated within host C_{2h}-**1** (Fig. 5b and S29–S31†). In addition, ESI-MS results exhibited a series of multicharged ions from $[Cd_8^{II}\mathbf{L}_4 + PFOA + 7NTf_2^- + KNO_3]^{8+}$ to $[Cd_8^{II}\mathbf{L}_4 + PFOA + 9NTf_2^- + KNO_3]^{6+}$, indicating the presence of host–guest complex PFOA⊂C_{2h}-**1** (Fig. S32†). That is, as the cavity of conformer D_2-**2** could not provide a suitable environment for PFOA, it transformed into conformer C_{2h}-**1** with the aim to accommodate the guest. Thus, the binding mechanism can be unambiguously assigned to conformational selection (Fig. 5a).

To further understand the mechanism of guest-induced conformational selection, theoretical calculations were conducted by using Forcite of Materials Studio (molecular-level interactions of the host–guest complex are shown in the ESI†). The calculated results are in good agreement with the experimental phenomenon, that is, the binding energy of host–guest complex PFOA⊂C_{2h}-**1** is −31.5 kcal mol^{-1}, which is more than that of PFOA⊂D_2-**2** ($\Delta E = -7.9$ kcal mol^{-1}) (Fig. S40–S42†). It's noted that the addition of PFOA into the solution of C_{2h}-**1** afforded the same result as PFOA⊂C_{2h}-**1**. In the ^{1}H and ^{19}F NMR titration experiments performed by continuously adding PFOA into C_{2h}-**1**, no free host C_{2h}-**1** was detected, suggesting PFOA's fast exchange binding model on the NMR timescale (Fig. S29†). The 1 : 1 host–guest stoichiometry was confirmed by the Job plot method (Fig. S33†).[60] The host–guest binding constant (K_a) was estimated by ^{1}H NMR titration and calculated to be 690 ± 20 M^{-1} based on Bindfit (Fig. S34†).[61]

Conclusions

We have presented a metallo-organic cube $Cd_8^{II}\mathbf{L}_4$ with two discrete conformations based on the different location

orientations of tetratopic ligand **L**. NMR, ESI-MS and SC-XRD techniques clearly supported the coexistence of two conformers. Time-resolved ^{1}H NMR spectra confirmed conformer C_{2h}-**1**'s extremely slow conversion to conformer D_2-**2**. Due to the different cavity volume and shape of the two conformers, a specific guest PFOA was selectively encapsulated by C_{2h}-**1**. Moreover, in the presence of PFOA, the conformational equilibrium between C_{2h}-**1** and D_2-**2** can be shifted to conformer C_{2h}-**1** with the aim to maximize the binding affinity. This host–guest behaviour strictly follows the conformation selection model, which can serve as a standard paradigm to study the deep mechanism of molecular recognition. In addition, the metallo-organic cube provides a suitable host, possessing the potential as a sorbent material and phase transfer or extraction system for the PFOA pollutant. Further studies will concentrate on improving the binding affinity through reasonable modifications of metallo-organic cubic cages.

Data availability

Crystallographic data for D_2-**2** have been deposited at the CCDC database under CCDC number 2359196† and can be obtained from The Cambridge Crystallographic Data Centre *via* **https://www.ccdc.cam.ac.uk/data_request/cif**. Further analytical data are reported in the ESI† to this article. Data are available upon request from the authors.

Author contributions

T. Wu and J. Z. conceived the study. Y.-Q. Li and Z. H. performed the synthesis. E. Han and Q. Bai performed characterization of the materials. Y.-M. Guan and Z. Zhang assisted in structural characterization (X-ray, NMR, and MS analyses). T. Wu wrote the original draft. P. Wang reviewed and edited the paper.

Conflicts of interest

There are no conflicts to declare.

Acknowledgements

We thank Dr Yi Huang (**https://www.castest.net**. No. Jin Tel: 400 096 8959) for the crystal structure determination and analysis in the work. This research was supported by the National Natural Science Foundation of China (22101061 and 22471047 to Z. Z. and 22401054 to T. W.), GuangDong Basic and Applied Basic Research Foundation (2023A1515110911 to T. W.), Guangzhou Basic and Applied Basic Research of City and University (Institute) Joint Funding Project (2023A03J0624 to P. W. and 2023A03J0023 to Z. Z.), and the Natural Science Foundation of Guangdong Province-Youth Enhancement Programme (2024A1515030235 to Z. Z.). The authors extend their gratitude to Theoretical and Computational Chemistry Team from Shiyanjia Lab (**https://www.shiyanjia.com**) for providing invaluable assistance.

Notes and references

1 R. Baron and J. A. McCammon, Molecular Recognition and Ligand Association, *Annu. Rev. Phys. Chem.*, 2013, **64**, 151–175.
2 E. Persch, O. Dumele and F. Diederich, Molecular recognition in chemical and biological systems, *Angew. Chem., Int. Ed.*, 2015, **54**, 3290–3327.
3 J. Monod, J. Wyman and J.-P. Changeux, On the nature of allosteric transitions: A plausible model, *J. Mol. Biol.*, 1965, **12**, 88–118.
4 D. D. Boehr, R. Nussinov and P. E. Wright, The role of dynamic conformational ensembles in biomolecular recognition, *Nat. Chem. Biol.*, 2009, **5**, 789–796.
5 H. Steuber, M. Zentgraf, C. L. Motta, S. Sartini, A. Heine and G. Klebe, Evidence for a Novel Binding Site Conformer of Aldose Reductase in Ligand-Bound State, *J. Mol. Biol.*, 2007, **369**, 186–197.
6 D. Ajami, L. Liu and J. Rebek Jr, Soft templates in encapsulation complexes, *Chem. Soc. Rev.*, 2015, **44**, 490–499.
7 D. M. Kaphan, M. D. Levin, R. G. Bergman, K. N. Raymond and F. D. Toste, A supramolecular microenvironment strategy for transition metal catalysis, *Science*, 2015, **350**, 1235–1238.
8 Z. Lu, T. K. Ronson, A. W. Heard, S. Feldmann, N. Vanthuyne, A. Martinez and J. R. Nitschke, Enantioselective fullerene functionalization through stereochemical information transfer from a self-assembled cage, *Nat. Chem.*, 2023, **15**, 405–412.
9 D. Fujita, Y. Ueda, S. Sato, N. Mizuno, T. Kumasaka and M. Fujita, Self-assembly of tetravalent Goldberg polyhedra from 144 small components, *Nature*, 2016, **540**, 563–566.
10 M. Yoshizawa and L. Catti, Bent Anthracene Dimers as Versatile Building Blocks for Supramolecular Capsules, *Acc. Chem. Res.*, 2019, **52**, 2392–2404.
11 L.-J. Wang, X. Li, S. Bai, Y.-Y. Wang and Y.-F. Han, Self-Assembly, Structural Transformation, and Guest-Binding Properties of Supramolecular Assemblies with Triangular Metal–Metal Bonded Units, *J. Am. Chem. Soc.*, 2020, **142**, 2524–2531.
12 T. Wu, Z. Jiang, Q. Bai, Y. Li, S. Mao, H. Yu, L. Wojtas, Z. Tang, M. Chen, Z. Zhang, T.-Z. Xie, M. Wang, X. Li and P. W, Supramolecular triangular orthobicupola: Self-assembly of a giant Johnson solid J_{27}, *Chem*, 2021, **7**, 2429–2441.
13 S. Sudan, F. Fadaei-Tirani, R. Scopelliti, K. E. Ebbert, G. H. Clever and K. Severin, $LiBF_4$-Induced Rearrangement and Desymmetrization of a Palladium-Ligand Assembly, *Angew. Chem., Int. Ed.*, 2022, **61**, e202201823.
14 B. Chen, J. J. Holstein, A. Platzek, L. Schneider, K. Wu and G. H. Clever, Cooperativity of steric bulk and H-bonding in coordination sphere engineering: heteroleptic Pd^{II} cages and bowls by design, *Chem. Sci.*, 2022, **13**, 1829–1834.
15 Q. Bai, Y.-M. Guan, T. Wu, Y. Liu, Z. Zhai, Q. Long, Z. Jiang, P. Su, T.-Z. Xie, P. Wang and Z. Zhang, Anion-Regulated Hierarchical Self-Assembly and Chiral Induction of

Metallo-Tetrahedra, *Angew. Chem., Int. Ed.*, 2023, **62**, e202309027.

16 A. C. Pearcy, L. S. Lisboa, D. Preston, N. B. Page, T. Lawrence, L. J. Wright, C. G. Hartinger and J. D. Crowley, Exploiting reduced-symmetry ligands with pyridyl and imidazole donors to construct a second-generation stimuli-responsive heterobimetallic $[PdPtL_4]^{4+}$ cage, *Chem. Sci.*, 2023, **14**, 8615–8623.

17 K. Wu, T. K. Ronson, P. Su, Z. Chen, L. Goh, A. W. Heard, X. Li, F. Klautzsch, C. A. Schalley, M. Vinković and J. R. Nitschke, Systematic construction of progressively larger capsules from a fivefold linking pyrrole-based subcomponent, *Nat. Synth.*, 2023, **2**, 789–797.

18 Y.-H. Huang, Y.-L. Lu, J. Ruan, S.-P. Zheng, X.-D. Zhang, C.-H. Liu, Y.-H. Qin, Z.-M. Cao, Z. Jiao, H.-S. Xu and C.-Y. Su, Dynamic Metallosupramolecular Cages Containing 12 Adaptable Pockets for High-Order Guest Binding Beyond Biomimicry, *J. Am. Chem. Soc.*, 2023, **145**, 23361–23371.

19 D. Zhang, T. K. Ronson, Y.-Q. Zou and J. R. Nitschke, Metal–organic cages for molecular separations, *Nat. Rev. Chem*, 2021, **5**, 168–182.

20 D. Chakraborty, R. Saha, J. K. Clegg and P. S. Mukherjee, Selective separation of planar and non-planar hydrocarbons using an aqueous Pd_6 interlocked cage, *Chem. Sci.*, 2022, **13**, 11764–11771.

21 D. Prajapati, J. K. Clegg and P. S. Mukherjee, Formation of a low-symmetry Pd_8 molecular barrel employing a hetero donor tetradentate ligand, and its use in the binding and extraction of C_{70}, *Chem. Sci.*, 2024, **15**, 12502–12510.

22 P. Howlader, B. Mondal, P. C. Purba, E. Zangrando and P. S. Mukherjee, Self-Assembled Pd(II) Barrels as Containers for Transient Merocyanine Form and Reverse Thermochromism of Spiropyran, *J. Am. Chem. Soc.*, 2018, **140**, 7952–7960.

23 A. J. Plajer, E. G. Percástegui, M. Santella, F. J. Rizzuto, Q. Gan, B. W. Laursen and J. R. Nitschke, Fluorometric Recognition of Nucleotides within a Water-Soluble Tetrahedral Capsule, *Angew. Chem., Int. Ed.*, 2019, **58**, 4200–4204.

24 M. Canton, A. B. Grommet, L. Pesce, J. Gemen, S. Li, Y. Diskin-Posner, A. Credi, G. M. Pavan, J. Andréasson and R. Klajn, Improving Fatigue Resistance of Dihydropyrene by Encapsulation within a Coordination Cage, *J. Am. Chem. Soc.*, 2020, **142**, 14557–14565.

25 E. Ubasart, O. Borodin, C. Fuertes-Espinosa, Y. Xu, C. García-Simón, L. Gómez, J. Juanhuix, F. Gándara, I. Imaz, D. Maspoch, M. von Delius and X. Ribas, A three-shell supramolecular complex enables the symmetry-mismatched chemo- and regioselective bis-functionalization of C_{60}, *Nat. Chem.*, 2021, **13**, 420–427.

26 W.-L. Jiang, B. Huang, X.-L. Zhao, X. Shi and H.-B. Yang, Strong halide anion binding within the cavity of a conformation-adaptive phenazine-based Pd_2L_4 cage, *Chem*, 2023, **9**, 2655–2668.

27 T. K. Piskorz, V. Martí-Centelles, R. L. Spicer, F. Duarte and P. J. Lusby, Picking the lock of coordination cage catalysis, *Chem. Sci.*, 2023, **14**, 11300–11331.

28 J. Gemen, M. J. Białek, M. Kazes, L. J. W. Shimon, M. Feller, S. N. Semenov, Y. Diskin-Posner, D. Oron and R. Klajn, Ternary host-guest complexes with rapid exchange kinetics and photoswitchable fluorescence, *Chem*, 2022, **8**, 2362–2379.

29 I. Heckelmann, Z. Lu, J. C. A. Prentice, F. Auras, T. K. Ronson, R. H. Friend, J. R. Nitschke and S. Feldmann, Supramolecular Self-Assembly as a Tool to Preserve the Electronic Purity of Perylene Diimide Chromophores, *Angew. Chem., Int. Ed.*, 2023, **62**, e202216729.

30 Z. Zhang, Q. Bai, Z. Zhai, Q. Long, E. Han, H. Zhao, C.-W. Zhou, H. Lin, W. Zhang, G.-H. Ning, T.-Z. Xie, P. Wang and T. Wu, Multiple-stimuli fluorescent responsive metallo-organic helicated cage arising from monomer and excimer emission, *Nat. Commun.*, 2024, **15**, 7261.

31 W. Wang, Y.-X. Wang and H.-B. Yang, Supramolecular transformations within discrete coordination-driven supramolecular architectures, *Chem. Soc. Rev.*, 2016, **45**, 2656–2693.

32 W. Liu and J. F. Stoddart, Emergent behavior in nanoconfined molecular containers, *Chem*, 2021, **7**, 919–947.

33 D.-N. Yan, L.-X. Cai, P.-M. Cheng, S.-J. Hu, L.-P. Zhou and Q.-F. Sun, Photooxidase Mimicking with Adaptive Coordination Molecular Capsules, *J. Am. Chem. Soc.*, 2021, **143**, 16087–16094.

34 X.-Q. Guo, L.-P. Zhou, S.-J. Hu, L.-X. Cai, P.-M. Cheng and Q.-F. Sun, Hexameric Lanthanide–Organic Capsules with Tertiary Structure and Emergent Functions, *J. Am. Chem. Soc.*, 2021, **143**, 6202–6210.

35 Y.-H. Huang, Y.-L. Lu, X.-D. Zhang, C.-H. Liu, J. Ruan, Y.-H. Qin, Z.-M. Cao, J. Jiang, H.-S. Xu and C.-Y. Su, Dynamic Stereochemistry of M_8Pd_6 Supramolecular Cages Based on Metal-Center Lability for Differential Chiral Induction, Resolution, and Recognition, *Angew. Chem., Int. Ed.*, 2023, **62**, e202315053.

36 D.-N. Yan, L.-X. Cai, S.-J. Hu, Y.-F. Zhou, L.-P. Zhou and Q.-F. Sun, An Organo-Palladium Host Built from a Dynamic Macrocyclic Ligand: Adaptive Self-Assembly, Induced-Fit Guest Binding, and Catalysis, *Angew. Chem., Int. Ed.*, 2022, **61**, e202209879.

37 E. Benchimol, B.-N. T. Nguyen, T. K. Ronson and J. R. Nitschke, Transformation networks of metal–organic cages controlled by chemical stimuli, *Chem. Soc. Rev.*, 2022, **51**, 5101–5135.

38 H.-Y. Lin, Y.-T. Wang, X. Shi, H.-B. Yang and L. Xu, Switchable metallacycles and metallacages, *Chem. Soc. Rev.*, 2023, **52**, 1129–1154.

39 Y. Domoto, M. Abe, G. R. Genov, Z. Yu and M. Fujita, Interconversion of Highly Entangled Polyhedra into Concave Polyhedra by Nitrate-Induced Ternary Coordination, *Angew. Chem., Int. Ed.*, 2023, **62**, e202303714.

40 N. M. A. Speakman, A. W. Heard and J. R. Nitschke, A $Cu^{I}_{6}L_{4}$ Cage Dynamically Reconfigures to Form Suit[4]anes and Selectively Bind Fluorinated Steroids, *J. Am. Chem. Soc.*, 2024, **146**, 10234–10239.
41 E. Fischer and J. D. Dermatol, Einfluss der Configuration auf die Wirkung der Enzyme, *Ges*, 1894, **27**, 2985–2993.
42 D. E. Koshland Jr, Application of a Theory of Enzyme Specificity to Protein Synthesis, *Proc. Natl. Acad. Sci. U.S.A.*, 1958, **44**, 98–104.
43 C. M. Hong, D. M. Kaphan, R. G. Bergman, K. N. Raymond and F. D. Toste, Conformational Selection as the Mechanism of Guest Binding in a Flexible Supramolecular Host, *J. Am. Chem. Soc.*, 2017, **139**, 8013–8021.
44 L.-P. Yang, L. Zhang, M. Quan, J. S. Ward, Y.-L. Ma, H. Zhou, K. Rissanen and W. Jiang, A supramolecular system that strictly follows the binding mechanism of conformational selection, *Nat. Commun.*, 2020, **11**, 2740.
45 T. K. Ronson, J. P. Carpenter and J. R. Nitschke, Dynamic optimization of guest binding in a library of diastereomeric heteroleptic coordination cages, *Chem*, 2022, **8**, 557–568.
46 R. Chakrabarty, P. S. Mukherjee and P. J. Stang, Supramolecular Coordination: Self-Assembly of Finite Two- and Three-Dimensional Ensembles, *Chem. Rev.*, 2015, **115**, 7001–7045.
47 T. R. Cook and P. J. Stang, Recent Developments in the Preparation and Chemistry of Metallacycles and Metallacages via Coordination, *Chem. Rev.*, 2015, **115**, 7001–7045.
48 S. Chakraborty and G. R. Newkome, Terpyridine-based metallosupramolecular constructs: tailored monomers to precise 2D-motifs and 3D-metallocages, *Chem. Soc. Rev.*, 2018, **47**, 3991–4016.
49 N. Fujita, K. Biradha, M. Fujita, S. Sakamoto and K. Yamaguchi, A Porphyrin Prism: Structural Switching Triggered by Guest Inclusion, *Angew. Chem., Int. Ed.*, 2001, **40**, 1718–1721.
50 G. Cecot, M. Marmier, S. Geremia, R. De Zorzi, A. V. Vologzhanina, P. Pattison, E. Solari, F. F. Tirani, R. Scopelliti and K. Severin, The Intricate Structural Chemistry of MII2nLn-Type Assemblies, *J. Am. Chem. Soc.*, 2017, **139**, 8371–8381.
51 G. J. Kleywegt and T. A. Jones, Detection, delineation, measurement and display of cavities in macromolecular structures, *Acta Crystallogr., Sect. D:Biol. Crystallogr.*, 1994, **50**, 178–185.
52 M. M. Renfrew, Drinking Water Health Advisory: Pesticides, *J. Chem. Educ.*, 1990, **67**, A55.
53 W. Ji, L. Xiao, Y. Ling, C. Ching, M. Matsumoto, R. P. Bisbey, D. E. Helbling and W. R. Dichtel, Removal of GenX and Perfluorinated Alkyl Substances from Water by Amine-Functionalized Covalent Organic Frameworks, *J. Am. Chem. Soc.*, 2018, **140**, 12677–12681.
54 M. Van den Bergh, A. Krajnc, S. Voorspoels, S. R. Tavares, S. Mullens, I. Beurroies, G. Maurin, G. Mali and D. E. De Vos, Highly Selective Removal of Perfluorinated Contaminants by Adsorption on All-Silica Zeolite Beta, *Angew. Chem., Int. Ed.*, 2020, **59**, 14086–14090.
55 M. J. Klemes, Y. Ling, C. Ching, C. Wu, L. Xiao, D. E. Helbling and W. R. Dichtel, Reduction of a Tetrafluoroterephthalonitrile-β-Cyclodextrin Polymer to Remove Anionic Micropollutants and Perfluorinated Alkyl Substances from Water, *Angew. Chem., Int. Ed.*, 2019, **58**, 12049–12053.
56 Z. Chen, Y.-L. Lu, L. Wang, J. Xu, J. Zhang, X. Xu, P. Cheng, S. Yang and W. Shi, Efficient Recognition and Removal of Persistent Organic Pollutants by a Bifunctional Molecular Material, *J. Am. Chem. Soc.*, 2023, **145**, 260–267.
57 Y. He, D. Luo, V. M. Lynch, M. Ahmed, J. L. Sessler and X. Chi, Porous adaptive luminescent metallacage for the detection and removal of perfluoroalkyl carboxylic acids, *Chem*, 2023, **9**, 93–101.
58 C. Dalvit and A. Vulpetti, Ligand-Based Fluorine NMR Screening: Principles and Applications in Drug Discovery Projects, *J. Med. Chem.*, 2019, **62**, 2218–2244.
59 Y. Yang, Y. Du, T. K. Ronson and J. R. Nitschke, Steric Control over Interligand Dihedrals and Splay Leads to the Formation of $Fe^{II}_{6}L_{6}$ and $Fe^{II}_{8}L_{8}$ Antiprisms, *CCS Chem.*, 2024, **6**, 2411–2419.
60 Z. Zhang, L. Ma, F. Fang, Y. Hou, C. Lu, C. Mu, Y. Zhang, H. Liu, K. Gao, M. Wang, Z. Zhang, X. Li and M. Zhang, Porphyrin-Based Multicomponent Metallacage: Host–Guest Complexation toward Photooxidation-Triggered Reversible Encapsulation and Release, *JACS Au*, 2022, **2**, 1479–1487.
61 C.-W. Zhou, X.-Z. Wang, M. Xie, R.-Q. Xia, D. Luo, Z.-X. Lian, G.-H. Ning, W. Lu, X.-P. Zhou and D. Li, A Self-Assembled Capsule for Propylene/Propane Separation, *Angew. Chem., Int. Ed.*, 2023, **62**, e202315020.